Tesque, Kyoto, Japan], 1 mM phenylmethylsulfonyl fluoride [PMSF] and protease inhibitor cocktail [Roche Diagnostics, Mannheim, Germany]), passed through a 26-gauge needle, allowed to stand on ice for 30 min before being centrifuged (16 000 *g* for 15 min). The supernatant (total cell lysate) was mixed with sodium dodecyl sulfate-polyacrylamide gel electrophoresis (SDS-PAGE) sample buffer (final: 125 mM Tris-HCl, pH 6.8, containing 5% glycerol, 2% SDS and 1% 2-mercaptoethanol), subjected to SDS-PAGE and electroblotted onto a polyvinylidene difluoride membrane (Bio-Rad, Hercules, CA, USA). Immunostaining was performed using primary antibodies against mouse iNOS (Affinity BioReagents, Golden, CO, USA); human phospho-IκBα (Ser32/36 [5A5]; Cell Signaling, Beverly, MA, USA); human IκBα and human IκBβ; mouse type I IL-1 receptor (IL-1RI) (Santa Cruz Biotechnology, Santa Cruz, CA, USA); and rat β-tubulin (internal control; Clone TUB2.1; Sigma Chemical Co., St. Louis, MO, USA), followed by visualization with an enhanced chemiluminescence (ECL) blotting detection reagent (GE Healthcare Biosciences Corp., Piscataway, NJ, USA).

For Akt, total cell lysates prepared from 100-mm dishes (5×10^6 cells/dish) were pre-cleared with Protein A (Sigma Chemical Co.) and then mixed with a mouse monoclonal antibody against human Akt1 (Akt5G3; Cell Signaling) and Protein G-Sepharose (Pharmacia LKB Biotech, Uppsala, Sweden). After incubation overnight at 4°C, immunocomplexes were centrifuged (16 000 *g* for 5 min). The beads were washed with solubilizing buffer, dissolved in SDS-PAGE sample buffer, and analyzed by western blotting using rabbit polyclonal antibodies against human Akt and phospho-(Ser473) Akt (Cell Signaling) as primary antibodies. In the case of p65, nuclear extracts were immunoprecipitated with an anti-p65 antibody (H286; Santa Cruz Biotechnology). The bands were analyzed by western blotting using an antibody against human NF-κB p65 (BD Transduction Laboratories, Lexington, KY, USA).

Reverse transcriptase-polymerase chain reaction

Total RNA was extracted from cultured hepatocytes using a guanidinium-phenol-chloroform method[19] with Trizol reagent (Invitrogen, Carlsbad, CA, USA) or a phenol-free, filter-based total RNA isolation kit (RNAqueous Kit; Ambion, Austin, TX, USA) according to the manufacturer's instructions, and then treated with a TURBO DNA-free Kit (Ambion) if necessary. For strand-specific reverse transcription-polymerase chain reaction (RT-PCR) analysis, cDNAs were synthesized from total RNA with strand-specific primers, and step-down PCR was performed using PC708 (Astec, Fukuoka, Japan), as previously described,[20,21] with minor modifications. For iNOS, IL-1RI, p65 and elongation factor-1α (EF; internal control) mRNAs, an oligo(dT) primer was used for RT and the primer sets 5′-CCAACCTGCAGGTCTTCGATG-3′ and 5′-GTCGATG CACAACTGGGTGAAC-3′ (257-bp product), 5′-CGAA GACTATCAGTTTTTGGAAC-3′ and 5′-GTCTTTCCATCT GAAGCTTTTGG-3′ (327-bp product), 5′-ACCCCTTTC AAGTTCCCATAGA-3′ and 5′-ACCTCAATGTCTTCTTTC TGCAC-3′ (262-bp product), and 5′-TCTGGTTGGAA TGGTGACAACATGC-3′ and 5′-CCAGGAAGAGCTTCA CTCAAAGCTT-3′ (307-bp product) were used for PCR, respectively. For the antisense-transcript of iNOS, the sense primer 5′-CCTTTGCCTCATACTTCCTCAGA-3′ was used for RT and the primer set 5′-ACCAGGAGGC GCCATCCCGCTGC-3′ and 5′-ATCTTCATCAAGGAATT ATACACGG-3′ (211-bp product) was used for PCR. The PCR protocols for iNOS, EF and IL-1RI were: 10 cycles of (94°C, 60 s; 72°C, 120 s); 15 cycles of (94°C, 60 s; 65°C, 90 s; 72°C, 20 s); and five (iNOS, EF) or 15 (IL-1R1) cycles of (94°C, 60 s; 60°C, 90 s; 72°C, 20 s). The PCR protocol for the antisense-transcript was: 10 cycles of (94°C, 60 s; 65°C, 90 s; 72°C, 20 s); 15 cycles of (94°C, 60 s; 60°C, 90 s; 72°C, 20 s); and five cycles of (94°C, 60 s; 55°C, 90 s; 72°C, 20 s). The amplified products were analyzed by 3% agarose gel electrophore-

Figure 1 Effects of kampo inchinkoto (TJ-135) on the induction of nitric oxide (NO) production and inducible nitric oxide synthase (iNOS) in pro-inflammatory cytokine-stimulated hepatocytes. Cultured hepatocytes were treated with interleukin-1β (IL-1β) (1 nM) in the presence or absence of TJ-135 (0.5–3.0 mg/mL). (a) Effect of TJ-135 (3 mg/mL) treatment (for the indicated times) on NO production (IL-1β, ○; IL-1β + TJ-135, ●; TJ-135, ▲; controls (without IL-1β and TJ-135), △). (b) Effects of treatment with various doses of TJ-135 (0.5–3.0 mg/mL) for 8 h on NO production. The levels of nitrite were measured in the culture medium (data are means ± standard deviation [SD], $n = 3$ dishes/point; $^*P < 0.05$ *vs.* IL-1β alone). (c) Cell lysates (20 μg of protein) were subjected to sodium dodecyl sulfate-polyacrylamide gel electrophoresis (SDS-PAGE) in a 7.5% gel, and immunoblotted with an anti-iNOS or anti-β-tubulin antibody. (d) Effects of TJ-135 (3 mg/mL) treatment (for the indicated times) on the expression of iNOS mRNA. Total RNA was analyzed by strand-specific reverse transcription-polymerase chain reaction (RT-PCR) to detect iNOS mRNA, using EF mRNA as an internal control.

sis with ethidium bromide, and the levels of iNOS, IL-1RI, EF and antisense-transcript were semi-quantified using a UV transilluminator. The cDNAs for the rat iNOS mRNA and antisense-transcript were deposited in the DNA Data Bank of Japan/European Bioinformatics Institute (DDBJ/EMBL)/GenBank under Accession numbers AB250951 and AB250952, respectively.

Electrophoretic mobility shift assay

Nuclear extracts were prepared as reported previously[22] with minor modifications.[23] Briefly, the dishes were placed on ice, washed with Tris-HCl-buffered saline, harvested into the same buffer using a rubber policeman and centrifuged (1840 *g* for 1 min). The precipitate (2×10^6 cells from two 35-mm dishes) was suspended in 400 μL of lysis buffer (10 mM Hepes, pH 7.9, 10 mM KCl, 0.1 mM EDTA, 0.1 mM EGTA, 500 U/mL trasylol, 0.5 mM PMSF and 1 mM dithiothreitol) and incubated on ice for 15 min. After addition of Nonidet P-40 (final: 0.625%), the cells were lysed by vortexing (two to three times for 1 min each) and centrifuged (15 000 *g* for 1 min). The nuclear pellet was resuspended in extraction buffer (10 mM Hepes, pH 7.9, 0.4 M NaCl, 0.1 mM EDTA, 0.1 mM EGTA, 500 U/mL trasylol, 0.5 mM PMSF and 1 mM dithiothreitol), followed by continuous mixing for 20 min and centrifugation (15 000 *g* for 5 min). Aliquots of the supernatant (nuclear extract) were frozen in liquid nitrogen and stored at −80 °C until use.

Binding reactions (total: 15 μL) were performed by incubating nuclear extract aliquots (4 μg of protein) in reaction buffer (20 mM Hepes, pH 7.9, 1 mM EDTA, 60 mM KCl, 10% glycerol and 1 mg of poly[dI-dC]) with the probe (approximately 40 000 cpm) for 20 min at room temperature. Products were electrophoresed at 100 V in a 4.8% polyacrylamide gel in high ionic strength buffer (50 mM Tris-HCl, 380 mM glycine, 2 mM EDTA, pH 8.5). Dried gels were analyzed by autoradiography. A NF-κB consensus oligonucleotide (5′-AGTTGAGGGGA-CTTTCCCAGGC-3′) from the mouse immunoglobulin κ light chain was purchased (Promega, Madison, WI, USA) and labeled with [γ-^{32}P]ATP and T4 polynucleotide kinase. The protein concentration was measured by the method of Bradford[24] with a binding assay kit (Bio-Rad) using bovine serum albumin as a standard.

Construction of luciferase reporter plasmids and expression plasmids

The 1.2-kb 5′-flanking region including the TATA box of the rat iNOS gene was inserted into the pGL3-Basic vector (Promega) to create pRiNOS-Luc-SVpA.[23] A rat cDNA for the 3′-untranslated region (UTR) of the iNOS mRNA was amplified with the primers 5′-tgctctaGAC AGTGAGGGGTTTGGAGAGA-3′ and 5′-gcggatcctttaTT CTTGATCAAACACTCATTTT-3′, and the resultant cDNA was digested with BamH I and Xba I. This cDNA for the iNOS 3′-UTR (submitted to DDBJ/EMBL/GenBank under Accession No. AB250951) was used to replace the SV40 polyadenylation signal (SVpA) of pRiNOS-Luc to create pRiNOS-Luc-3′UTR.

Transfection and luciferase assay

Transfection of cultured hepatocytes was performed as described previously.[25,26] Briefly, hepatocytes were cultured at 4×10^5 cells/dish (35 × 10 mm) in WE supplemented with serum, dexamethasone and insulin for 7 h, before being subjected to magnet-assisted transfection (MATra). Reporter plasmids pRiNOS-Luc-SVpA or pRiNOS-Luc-3′UTR (1 μg) and the CMV promoter-driven β-galactosidase plasmid pCMV-LacZ (1 ng) as an internal control were mixed with MATra-A reagent (1 μL; IBA GmbH, Göttingen, Germany). After incubation for 15 min on a magnetic plate at room temperature, the medium was replaced with fresh WE containing serum. Cells were cultured overnight, and then treated with IL-1β in the presence or absence of sivelestat. The luciferase and β-galactosidase activities of cell extracts were measured using PicaGene (Wako Pure Chemicals) and Beta-Glo (Promega) kits, respectively.

Statistical analysis

Results shown are representative of three to four independent experiments yielding similar findings.

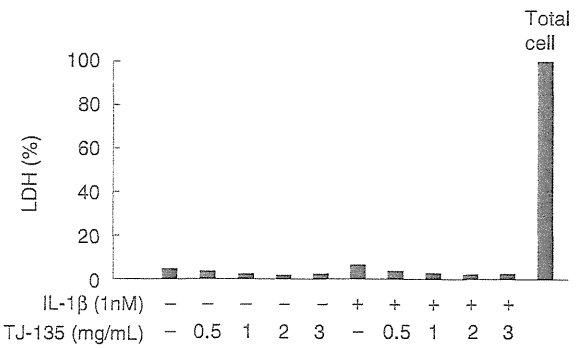

Figure 2 Effects of kampo inchinkoto (TJ-135) on cellular cytotoxicity. Cells were treated with IL-1β (1 nM) in the presence or absence of TJ-135 (0.5–3.0 mg/mL) for 8 h. Lactate dehydrogenase (LDH) activity was measured in the culture medium (data are means ± standard deviation [SD], $n = 3$ dishes/point).

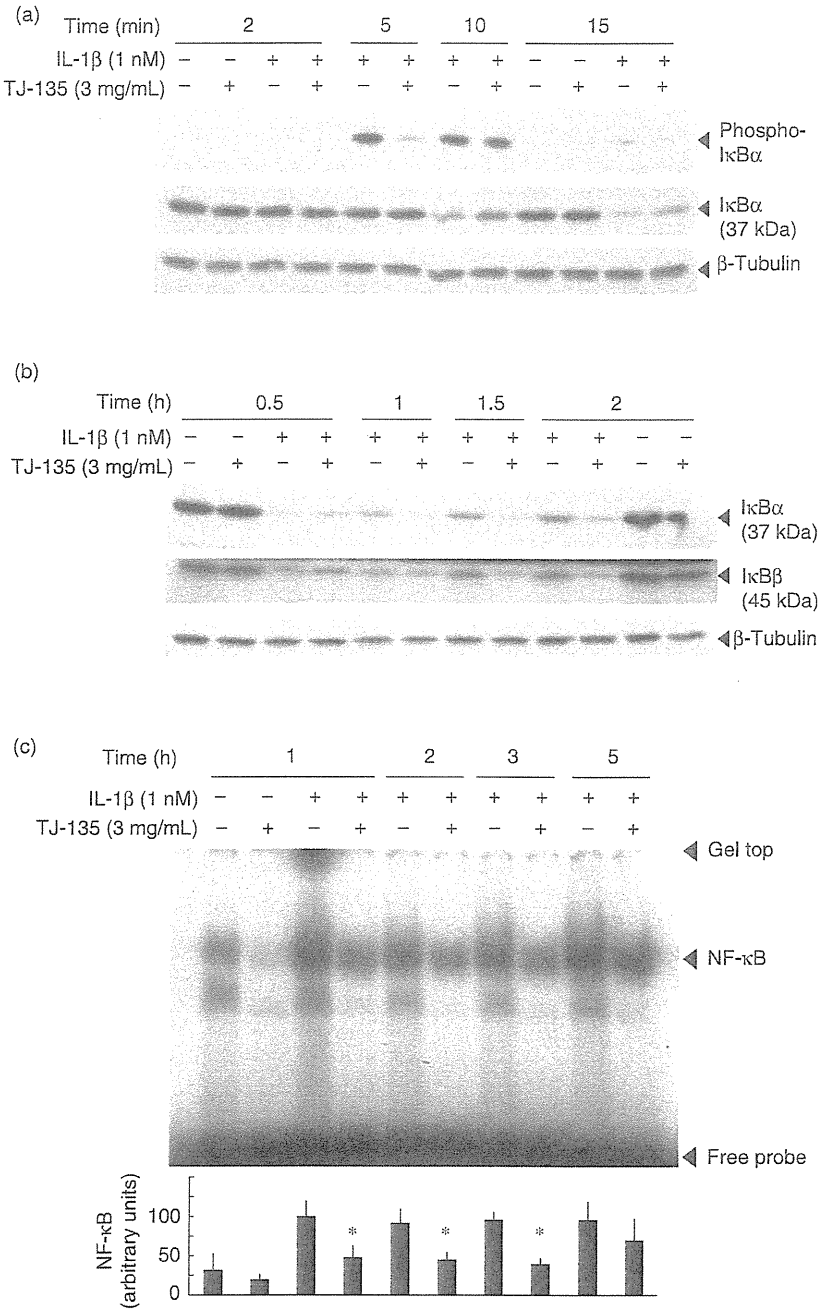

Figure 3 Effects of kampo inchinkoto (TJ-135) on the degradation of IκB proteins and activation of nuclear factor-κB (NF-κB). Cells were treated with interleukin-1β (IL-1β) (1 nM) in the presence or absence of TJ-135 (3 mg/mL) for the indicated times. (a, b) Cell lysates (20 μg of protein) were subjected to sodium dodecyl sulfate-polyacrylamide gel electrophoresis (SDS-PAGE) in a 12.5% gel, followed by immunoblotting with an anti-phospho-IκBα, anti-IκBα, anti-IκBβ or anti-β-tubulin antibody. (c) Activation of NF-κB. Nuclear extracts (4 μg of protein) were analyzed by electrophoretic mobility shift assay (EMSA) (upper). The bands corresponding to NF-κB were quantified by densitometry (lower, means ± standard deviation (SD) for $n = 3$ experiments; $^*P < 0.05$ *vs.* IL-1β alone). (d) Nuclear translocation of NF-κB subunit p65. Nuclear extracts were immunoprecipitated, and the immunoprecipitates were analyzed by western blotting with an anti-p65 antibody. (e) Total RNA was analyzed by strand-specific reverse transcription-polymerase chain reaction (RT-PCR) to detect p65 mRNA, using elongation factor (EF) mRNA as an internal control.

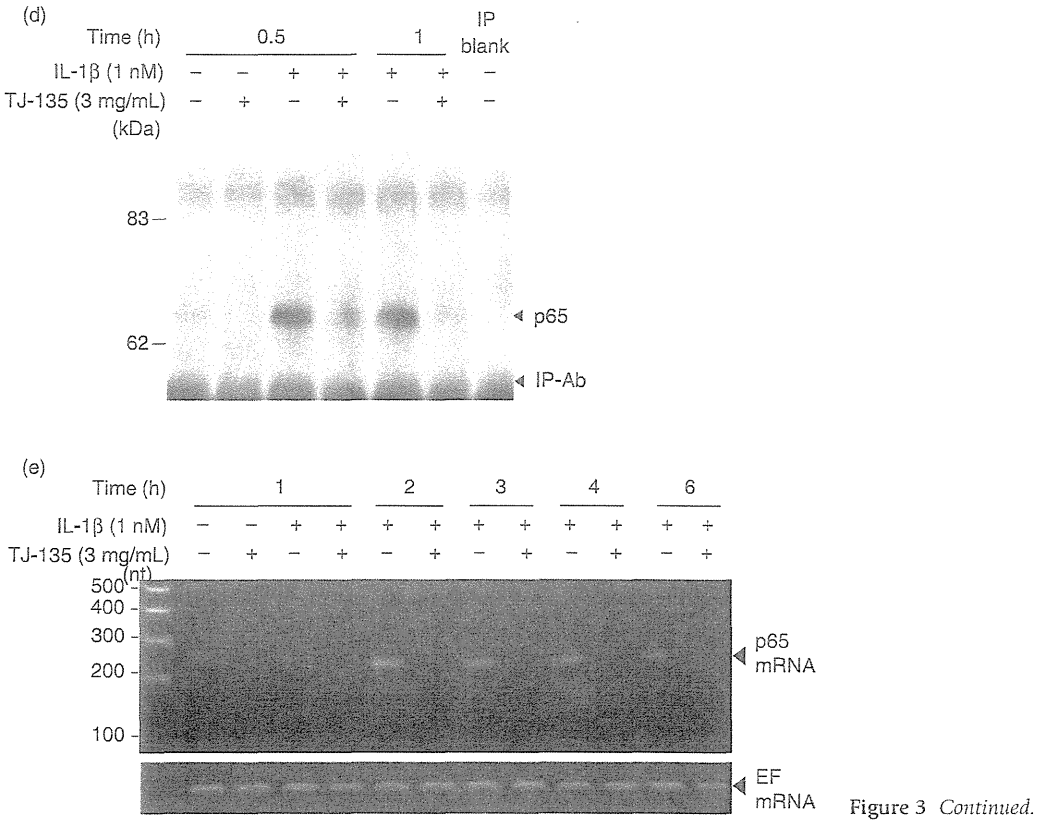

Figure 3 *Continued.*

Differences were analyzed by the Bonferroni-Dunn test, and values of $P < 0.05$ were considered to indicate statistical significance.

RESULTS

Effects of TJ-135 on the induction of NO production and iNOS in IL-1β-stimulated hepatocytes

THE PROINFLAMMATORY CYTOKINE IL-1β stimulates the induction of iNOS, which is followed by the production of NO in primary cultured rat hepatocytes.[27,28] Simultaneous addition of TJ-135 with IL-1β time- and dose-dependently reduced the levels of nitrite (a NO metabolite) in the culture medium (Fig. 1a,b). TJ-135 exerted its maximal effects at the concentration of 3 mg/mL, decreasing NO production to near basal levels. TJ-135 showed no cellular cytotoxicity within the indicated concentrations, as evaluated by the release of LDH into the culture medium (Fig. 2) and Trypan blue exclusion by hepatocytes (data not shown). Western blotting analysis revealed that TJ-135 time- and dose-dependently decreased the levels of iNOS protein expression, showing its maximal effect at 3 mg/mL (Fig. 1c). RT-PCR analysis revealed that TJ-135 decreased the levels of iNOS mRNA expression (Fig. 1d). These results suggested that TJ-135 inhibited the induction of iNOS gene expression at a transcriptional and/or post-transcriptional step.

Effects of TJ-135 on NF-κB activation and IL-1RI upregulation

We examined the mechanisms involved in the inhibition of iNOS induction. IL-1β stimulates the degradation of IκB proteins after the phosphorylation by IκB kinase, which is followed by the activation of NF-κB (i.e. translocation from the cytoplasm to the nucleus, and DNA binding). TJ-135 had no effect on the degradation of IκBα at 10–15 min (Fig. 3a, middle), and although TJ-135 reduced IκBα phosphorylation after 5 min of IL-1β stimulation, it had no

effect on phosphorylation levels at 10 min (Fig. 3a, top). In addition, TJ-135 did not inhibit the degradation of IκBα and IκBβ at 0.5 h, and rather decreased their recovery at one hour and thereafter (Fig. 3b). In contrast, electrophoretic mobility shift assays (EMSAs) with nuclear extracts revealed that TJ-135 inhibited NF-κB activation at 1–5 h (Fig. 3c), although the difference at 5 h was not significant. In support of this observation, immunoprecipitation and western blotting of nuclear extracts showed that TJ-135 decreased the levels of NF-κB subunit p65 in the nucleus (Fig. 3d). Furthermore, TJ-135 decreased the levels of p65 mRNA expression (Fig. 3e).

Interleukin-1β also stimulates the upregulation of IL-1RI through the activation of phosphatidylinositol 3-kinase (PI3K)/Akt. Immunoprecipitation-western blotting analysis revealed that TJ-135 inhibited the phosphorylation (activation) of Akt, a downstream kinase of PI3K (Fig. 4a). RT-PCR and western blot analyses revealed that TJ-135 reduced the levels of IL-1RI mRNA and protein expression (Fig. 4b,c).

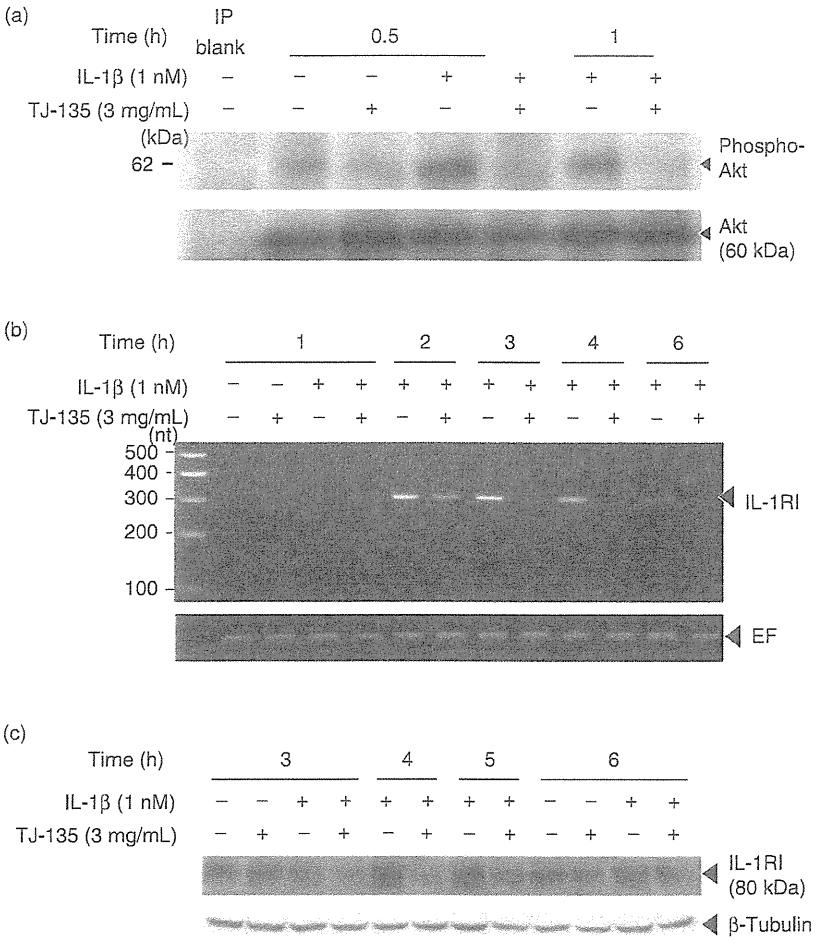

Figure 4 Effects of kampo inchinkoto (TJ-135) on the upregulation of IL-1RI. Cells were treated with IL-1β (1 nM) in the presence or absence of TJ-135 (3 mg/mL) for the indicated times. (a) Phosphorylation of Akt. Total cell lysates were immunoprecipitated with an anti-Akt antibody, followed by immunoblotting with an anti-phospho-Akt or anti-Akt antibody. (b) Total RNA was analyzed by strand-specific reverse transcription-polymerase chain reaction (RT-PCR) to detect IL-1RI mRNA, using elongation factor (EF) mRNA as an internal control. (c) Cell lysates (50 μg of protein) were subjected to sodium dodecyl sulfate-polyacrylamide gel electrophoresis (SDS-PAGE) in a 7.5% gel, and immunoblotted with an anti-IL-1RI or anti-β-tubulin antibody.

Effects of TJ-135 on iNOS promoter activation and its mRNA stabilization

Next, we carried out transfection experiments with constructs containing firefly luciferase controlled by the iNOS promoter (pRiNOS-Luc-SVpA and pRiNOS-Luc-3'UTR) (Fig. 5a), which detect iNOS promoter transactivation (mRNA synthesis) and mRNA stabilization, respectively.[29] IL-1β increased the luciferase activities of these constructs, an effect significantly inhibited by TJ-135 (Fig. 5b,c). Furthermore, iNOS antisense-transcript analysis by RT-PCR revealed that IL-1β

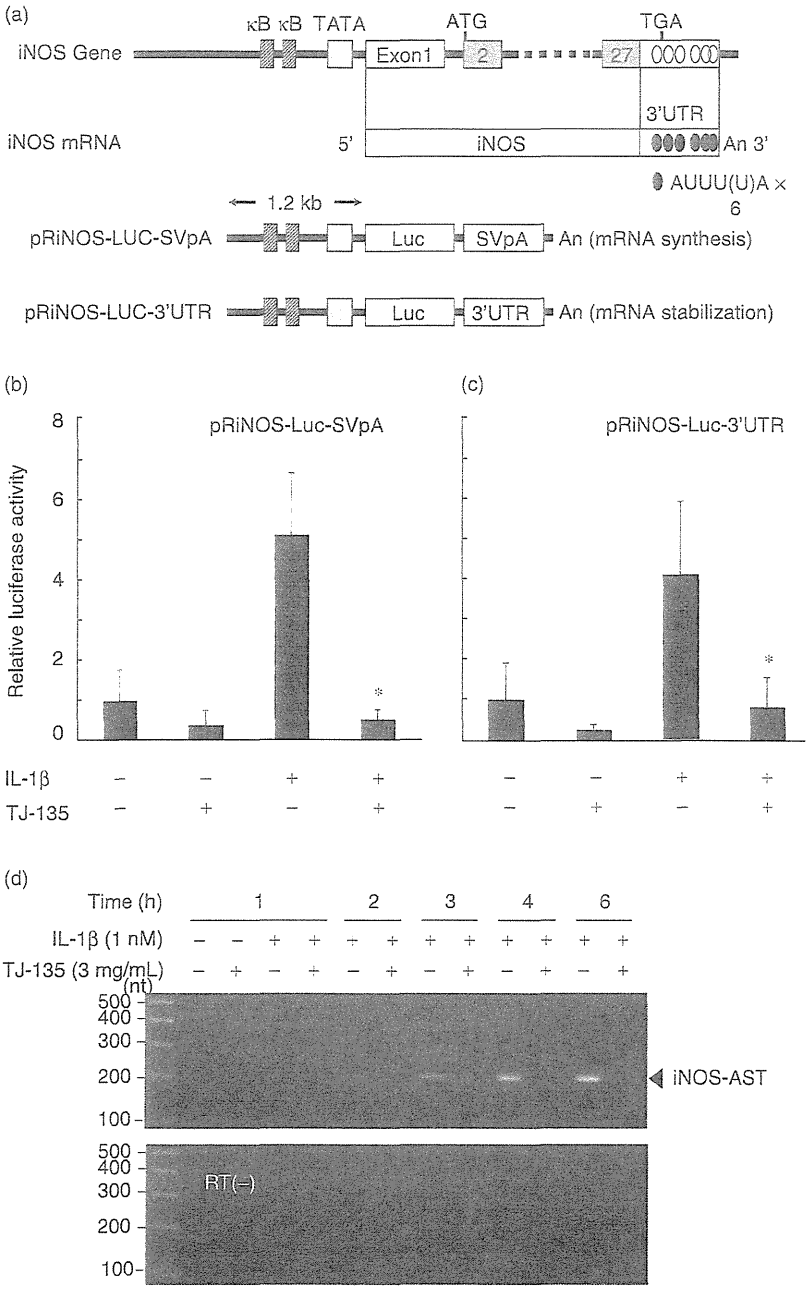

Figure 5 Effects of kampo inchinkoto (TJ-135) on the transactivation of the inducible nitric oxide synthase (iNOS) promoter and the expression of the iNOS gene antisense-transcript. (a) Schematic representation of the promoter region of the iNOS gene. Two reporter constructs are shown beneath the iNOS gene and mRNA. The constructs consist of the rat iNOS promoter (1.2 kb), a luciferase gene and the SV40 poly(A) region (pRiNOS-Luc-SVpA) or iNOS 3'-UTR (pRiNOS-Luc-3'UTR). "A_n" indicates the presence of a poly(A) tail. The iNOS 3'-UTR contains AREs (AUUU(U)A × 6), which contribute to mRNA stabilization. (b, c) Each construct was introduced into hepatocytes, and the cells were treated with interleukin-1β (IL-1β) (1 nM) in the presence or absence of TJ-135 (3 mg/mL) for 8 h for pRiNOS-Luc-SVpA (B) and 4 h for pRiNOS-Luc-3'UTR (C). The luciferase activities were normalized to β-galactosidase activity. The fold activation was calculated by dividing the luciferase activity by the control activity (without IL-1β and TJ-135). Data are means ± standard deviation [SD], $n = 4$ dishes. $^*P < 0.05$ *vs.* IL-1β alone. (d) Cells were treated with IL-1β (1 nM) in the presence or absence of TJ-135 (3 mg/mL) for the indicated times. Total RNA was analyzed by strand-specific reverse transcription-polymerase chain reaction (RT-PCR) to detect the iNOS gene antisense-transcript (AST). RT(–) denotes a negative control PCR using total RNA without RT.

increased the expression of the iNOS gene antisense-transcript in a time-dependent manner, and that TJ-135 markedly inhibited this effect (Fig. 3d).

Effects of delayed administration or withdrawal of TJ-135 on iNOS induction

We examined whether delayed administration of TJ-135 influences iNOS induction. TJ-135 was added to the medium 1–4 h after the addition of IL-1β. Although the magnitude of inhibition decreased time-dependently, delayed administration of TJ-135 up to 4 h after IL-1β addition still markedly inhibited NO production (Fig. 6). We then studied whether TJ-135 is effective even if it is not present in the medium for the entire experimental duration. We compared the time course of IL-1β-stimulated NO production in the absence of TJ-135 with that seen when TJ-135 was added 3 h after IL-1β addition (3 h delay of TJ-135) and when TJ-135 was washed out for 3 h after initial co-administration of TJ-135 and IL-1β (3 h withdrawal of TJ-135). As shown in Figure 7a, even after a 3 h delay prior to addition, TJ-135 inhibited approximately 70% of NO production. Similarly, after withdrawal of TJ-135 for 3 h after co-administration with IL-1β, NO production was inhibited by more than 90% compared with the level of production seen with IL-1β alone. The 3 h delay of TJ-135 decreased the levels of iNOS protein but not as effectively after the 3 h withdrawal of TJ-135 (Fig. 7b). However, both delay and withdrawal of TJ-135 had similar inhibitory effects on the expression of iNOS mRNA and its antisense-transcript (7C and 7D), the activation of NF-κB (Fig. 7e) and the nuclear translocation of NF-κB subunit p65 (Fig. 7f).

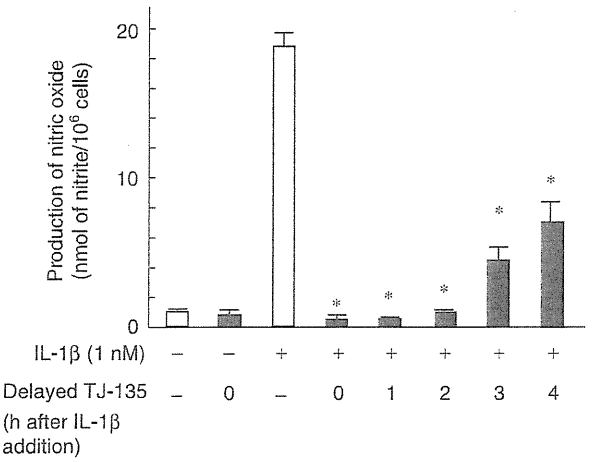

Figure 6 Effects of delayed kampo inchinkoto (TJ-135) administration on the production of nitric oxide (NO) in hepatocytes. Cultured hepatocytes were treated with TJ-135 (3 mg/mL) at 0–4 h after the addition of interleukin-1β (IL-1β) (1 nM). The effects of TJ-135 on NO production were analyzed at 8 h after IL-1β addition. The levels of nitrite were measured in the culture medium (data are means ± standard deviation [SD], $n = 3$ dishes/point; $^*P < 0.05$ *vs.* IL-1β alone).

Effects of TJ-135 components on NO production and the induction of iNOS

We examined the effects of the three components of TJ-135 on the production of NO and expression of iNOS protein. As shown in Figure 8, the extract of *A. capillaris* dose-dependently inhibited NO production ($ED_{50} = 0.53$ mg/mL) and iNOS protein expression in IL-1β-stimulated hepatocytes. This effect was of similar magnitude as with complete TJ-135. The extract of *G. fructus* also dose-dependently decreased NO production ($ED_{50} = 1.67$ mg/mL) but less effectively than *A. capillaris*. The extracts of *A. capillaris* and *G. fructus* showed no cellular cytotoxicity at the indicated concentrations, as evaluated by LDH release into the medium (data not shown). The extract of *R. rhizome* had inhibitory effects at 0.25 and 0.5 mg/mL, but showed cytotoxicity at concentrations of 1 mg/mL and above.

DISCUSSION

IN THE PRESENT study, we found that Kampo inchinkoto, TJ-135, inhibited iNOS induction, followed by the reduction of NO production in IL-1β-stimulated hepatocytes (Fig. 1a–d). It is known that the levels of iNOS mRNA are regulated by iNOS promoter transactivation under the control of transcription factors such as NF-κB and by posttranscriptional modifications such as mRNA stabilization.[30] In experiments with iNOS promoter constructs, TJ-135 was found to inhibit iNOS induction at both the mRNA synthesis and stabilization phases (Fig. 5). During mRNA synthesis, TJ-135 probably reduced the transactivation of the iNOS promoter (Fig. 5b) through the inhibition of NF-κB activation (Fig. 3c), although TJ-135 had no effect on IκBα and IκBβ degradation (Fig. 3a,b). NF-κB typically exists in the form of p50/65 heterodimers attached to its inhibitory proteins (IκBs, IκBα and IκBβ) in the cytoplasm of cells. The activation of NF-κB involves (i) proteolytic degradation of IκBs in proteosome after the phosphorylation by IκB kinase (ii) the translocation of NF-κB to the nucleus, and (iii) its binding to the promoter κB

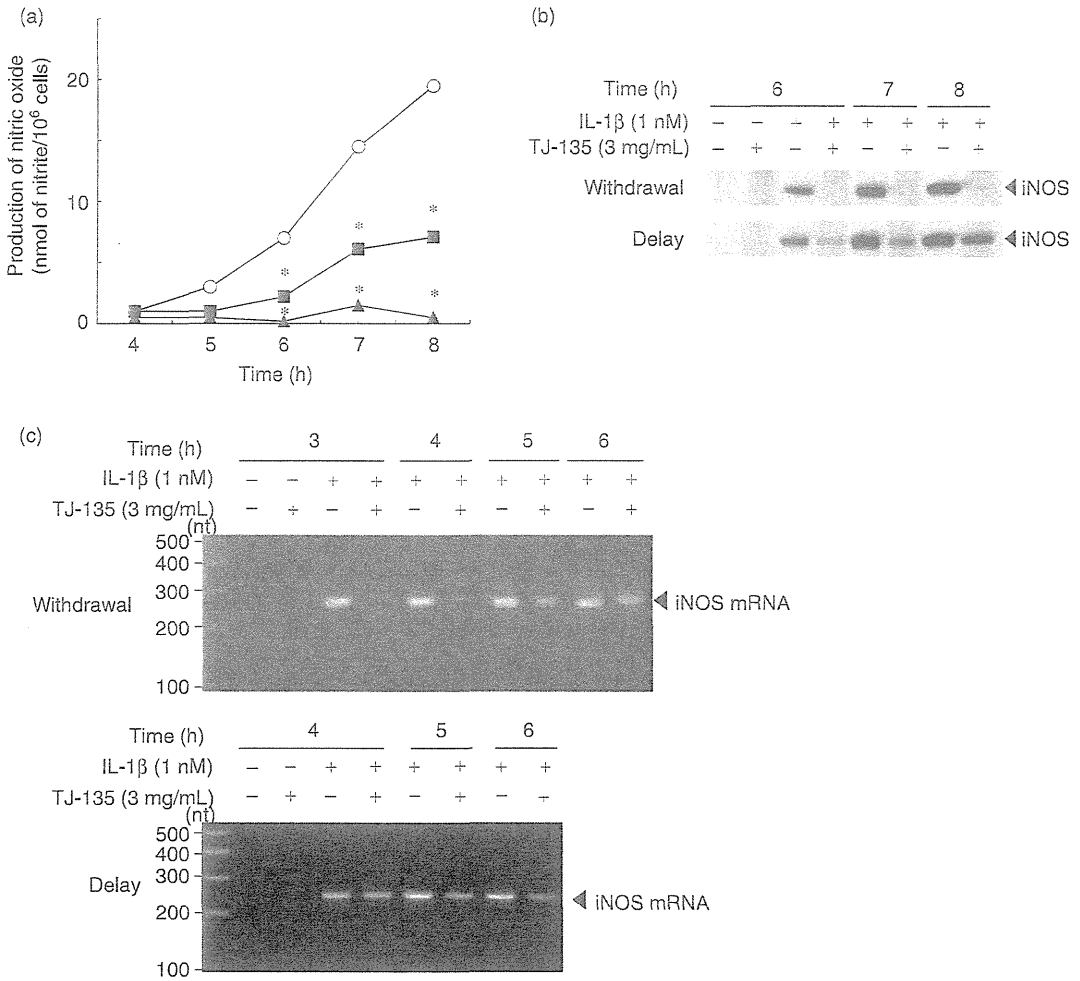

Figure 7 Effects of delayed administration and withdrawal of kampo inchinkoto (TJ-135) on the induction of inducible nitric oxide synthase (iNOS) in hepatocytes. Cultured hepatocytes were treated with TJ-135 (3 mg/mL) at 3 h after the addition of interleukin-1β (IL-1β) (1 nM) (3 h delay) or treated with simultaneous addition of IL-1β and TJ-135, followed by the withdrawal of TJ-135 at 3 h (3 h withdrawal). The effects of TJ-135 on IL-1β-stimulated nitric oxide (NO) production (a), iNOS protein expression (b), iNOS mRNA expression (c), iNOS antisense-transcript expression (d), nuclear factor-κB (NF-κB) levels (e) and nuclear translocation of NF-κB subunit p65 (f) were analyzed at the indicated times after IL-1β addition. (a) The levels of nitrite (IL-1β, ○; IL-1β + TJ-135 (3 h delay), ■; IL-1β + TJ-135 (3 h withdrawal), ▲) were measured in the culture medium (data are means ± standard deviation [SD], $n = 3$ dishes/point; $^*P < 0.05$ *vs.* IL-1β alone). (b) Cell lysates (20 μg of protein) from cells stimulated as described above were subjected to sodium dodecyl sulfate-polyacrylamide gel electrophoresis (SDS-PAGE) in a 7.5% gel, and immunoblotted with an anti-iNOS or anti-β-tubulin antibody. (c, d) Total RNA was analyzed by strand-specific reverse transcription-polymerase chain reaction (RT-PCR (to detect iNOS mRNA, using EF mRNA as an internal control, and the iNOS gene antisense-transcript (AST). (e) Nuclear extracts (4 μg of protein) from cells stimulated as described above were analyzed by electrophoretic mobility shift assay (EMSA). (f) Nuclear extracts were immunoprecipitated, and these precipitates were analyzed by western blotting using an anti-p65 antibody. W, 3 h withdrawal of TJ-135; D, 3 h delay of TJ-135.

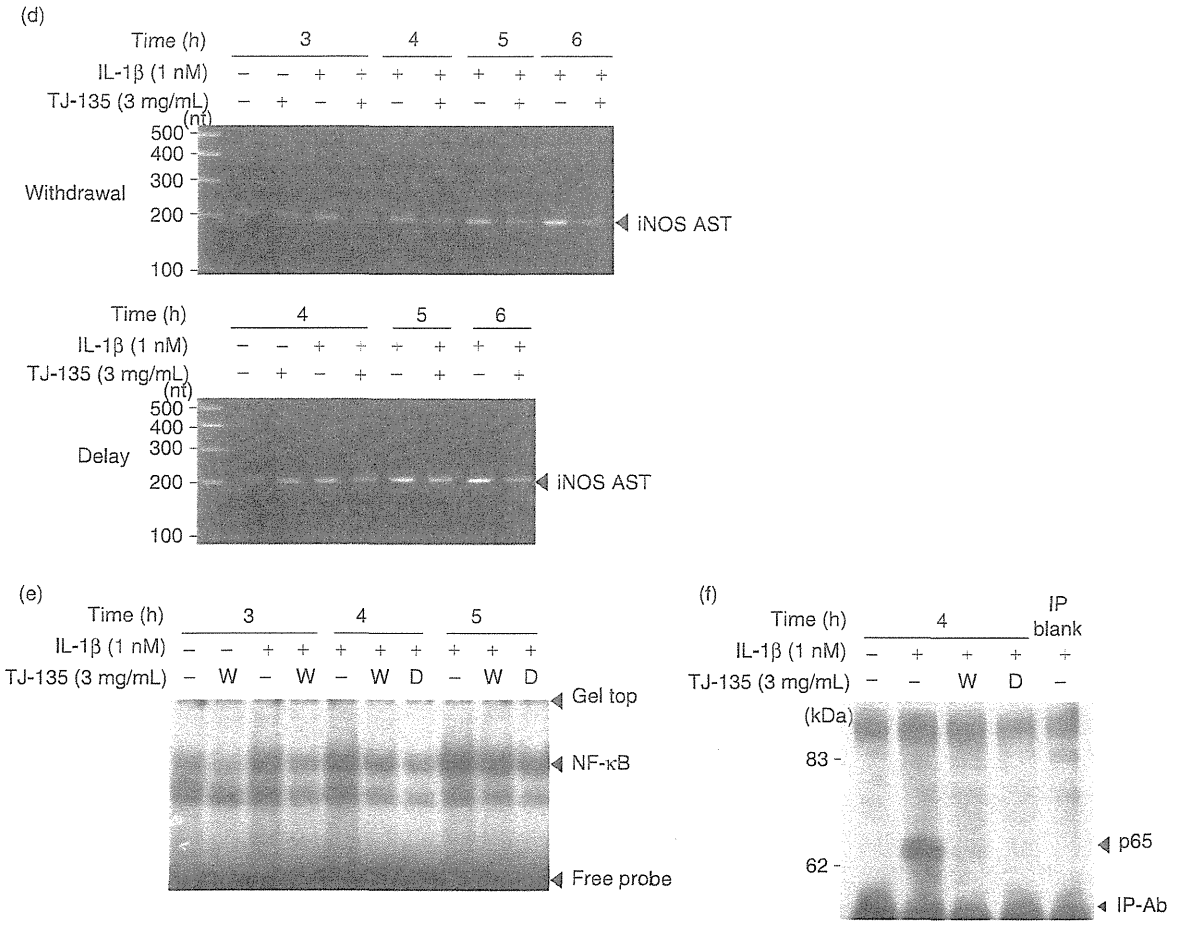

Figure 7 *Continued.*

site.[31] TJ-135 inhibited the translocation of p65 to the nucleus (Fig. 3d) at least partly by decreasing p65 mRNA expression (Fig. 3e).

In addition to the activation of NF-κB through IκB degradation, the upregulation of IL-1RI through the activation of PI3K/Akt is also essential for iNOS induction.[32] IL-1β stimulates the induction of IL-1RI, which precedes the induction of iNOS. The upregulation of IL-1RI is associated with a second activation of Akt, which accelerates the phosphorylation of the NF-κB p65 subunit and increases the transcriptional activation of the iNOS gene. In the present study, we found that TJ-135 decreased the expression of IL-1RI mRNA and protein (Fig. 4b,c) through the inhibition of Akt phosphorylation (Fig. 4a), which is presumably also involved in the observed decrease in iNOS promoter transactivation activity.

Regarding iNOS mRNA stabilization, the 3′-UTR of the iNOS mRNA in rats has six AREs (AUUUU(U)A), which are associated with ARE-binding proteins such as HuR and heterogeneous nuclear ribonucleoproteins L/I (PTB), which serve to stabilize the mRNA.[33] Recently, we found that the antisense strand corresponding to the 3′-UTR of the iNOS mRNA is transcribed from the iNOS gene, and that the iNOS mRNA antisense-transcript plays a key role in stabilizing the iNOS mRNA by interacting with the 3′-UTR and ARE-binding proteins.[34] In our *in vitro* model, TJ-135 destabilized the iNOS mRNA by inhibiting iNOS gene antisense-transcript expression (Fig. 3d). Drugs such as edaravone (free radical scavenger),[14] FR183998 (Na^+/H^+ exchanger inhibitor),[10,12] insulin growth factor I[11] and sivelestat[35] were found to inhibit iNOS induction partly by suppressing iNOS antisense-transcript

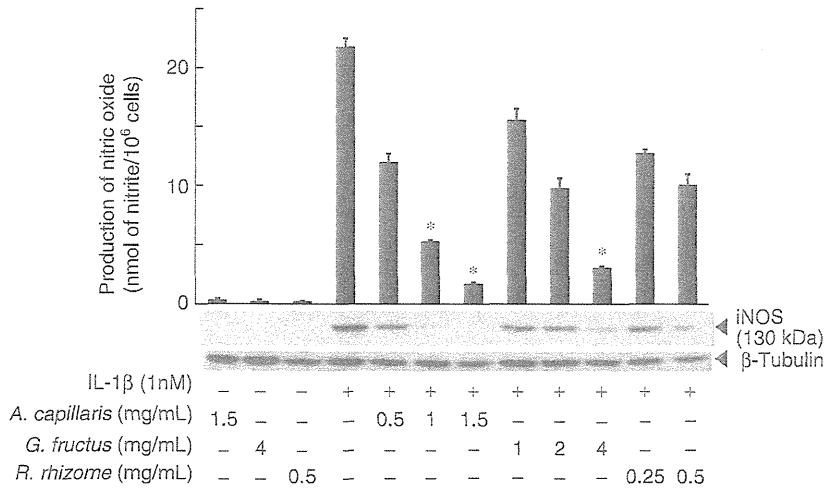

Figure 8 Effects of the three components of kampo inchinkoto (TJ-135) on nitric oxide (NO) production and inducible nitric oxide synthase (iNOS) induction. Cultured hepatocytes were treated with IL-1β (1 nM) for 8 h in the presence or absence of extracts from *A. capillaris* (0.5–1.5 mg/mL), *Gardenia fructus* (1–4 mg/mL) and *Rhei rhizome* (0.25–0.5 mg/mL). The levels of nitrite were measured in the culture medium (data are means ± standard deviation [SD], $n = 3$ dishes/point; $^*P \leq 0.05$ *vs.* IL-1β alone). In the western blotting panels, cell lysates (20 μg of protein) were subjected to sodium dodecyl sulfate-polyacrylamide gel electrophoresis (SDS-PAGE) in a 7.5% gel, and immunoblotted with an anti-iNOS or anti-β-tubulin antibody.

production in animal models of liver injury and primary cultured hepatocytes.

Delayed treatment with TJ-135 or withdrawal of TJ-135 after IL-1β addition was found to cause a significant reduction in NO production and iNOS protein expression (Figs 6,7a,b). The fact that a delay in initiating treatment does not abrogate the effects of the drug may be of clinical importance, since TJ-135 treatment is not usually administered at the precise moment of disease onset. In the case of the 3 h withdrawal treatment, TJ-135 reduced the levels of NO production and iNOS protein expression to the same extent as TJ-135 addition without withdrawal. We concluded that delayed treatment with TJ-135, unlike withdrawal treatment, could not influence the IL-1β-stimulated, Akt-driven expression of IL-1RI mRNA, since these events are almost complete at 3 h (Fig. 4a,b). The resultant inhibition of iNOS induction will therefore be smaller. However, we found that both delayed and withdrawal treatments reduced the expression of iNOS mRNA and its antisense-transcript to similar levels (Fig. 7c,d). These treatments were also equi-effective at inhibiting NF-κB activation (Fig. 7e) and nuclear translocation of p65 (Fig. 7f). We cannot therefore rule out the possibility that TJ-135 may affect iNOS induction at a translational step by inhibiting IL-1RI upregulation *via* the PI3K/Akt pathway.

Recently, Kawai *et al.*[36] have reported that preoperative administration of inchinkoto exerts beneficial effects in rat liver with ischemia-reperfusion and subsequent hepatectomy, where inchinkoto attenuated ischemia-reperfusion injury-induced mortality. They demonstrated that inchinkoto reduced the upregulation of genes for inflammatory cytokines and iNOS, and increased levels of liver nitrotyrosine. Nitrotyrosine is an oxidative product of peroxynitrite formed by excess NO, and is a marker of NO-dependent damage *in vivo*. We found that all three components in inchinkoto, *A. capillaris*, *G. fructus* and *R. rhizome*, are involved in the inhibitory effect of TJ-135 on NO production, where *A. capillaris* contributes most significantly to the effect of TJ-135 (Fig. 8). We also found that genipin, the major ingredient of *G. fructus* and an aglycone converted in the gut by intestinal bacteria from geniposide,[37] inhibited the induction of iNOS (T. Matsuura and T. Okumura, unpubl. data, 2010). Genipin was also found to reduce iNOS in a rat model of ischemia-reperfusion injury.[36]

In conclusion, TJ-135 inhibited the induction of iNOS gene expression through the inhibition of its promoter transactivation and mRNA stabilization in pro-inflammatory cytokine-stimulated hepatocytes, a simple *in vitro* liver injury model. TJ-135 may have therapeutic

potential for a variety of organ injuries including acute liver dysfunction by suppressing iNOS induction.

REFERENCES

1 Arai M, Yokosuka O, Fukai K *et al.* A case of severe acute hepatitis of unknown etiology treated with the Chinese herbal medicine Inchinko-to. *Hepatol Res* 2004; 28: 161–5.
2 Ohwada S, Kobayashi I, Hasegawa N, Tsuda K, Inui Y. Severe acute cholistatic hepatitis of unknown etiology successfully treated with the Chinese herbal medicine Inchinko-to (TJ-135). *World J Gastroenterol* 2009; 15: 2927–9.
3 Okada K, Shoda J, Kano M *et al.* Inchinkoto, a herbal medicine, and its ingredients dually exert Mrp2/MRP2-mediated choleresis and Nrf2-mediated antioxidative action in rat livers. *Am J Physiol Gastrointest Liver Physiol* 2007; 292: G1450–63.
4 Shoda J, Miura T, Utsunomiya H *et al.* Genipin enhances Mrp2 (Abcc2)-mediated bile formation and organic anion transport in rat liver. *Hepatology* 2004; 39: 167–78.
5 Ikeda H, Nagashima K, Yanase M *et al.* The herbal medicine inchin-ko-to (TJ-135) induces apoptosis in cultured rat hepatic stellate cells. *Life Sci* 2006; 78: 2226–33.
6 Inao M, Mochida S, Matsui A *et al.* Japanese herbal medicine Inchin-ko-to as a therapeutic drug for liver fibrosis. *J Hepatol* 2004; 41: 584–91.
7 Colasanti M, Suzuki H. The dual personality of NO. *Trends Pharmacol Sci* 2000; 21: 249–52.
8 Tsuchiya H, Kaibori M, Yanagida H *et al.* Pirfenidone prevents endotoxin-induced liver injury after partial hepatectomy in rats. *J Hepatol* 2004; 40: 94–101.
9 Tsuji K, Kwon A-H, Yoshida H *et al.* Free radical scavenger (edaravone) prevents endotoxin-induced liver injury after partial hepatectomy in rats. *J Hepatol* 2005; 42: 94–101.
10 Tanaka H, Uchida Y, Kaibori M *et al.* Na^+/H^+ exchanger inhibitor, FR183998, has protective effect in lethal acute liver failure and prevents iNOS induction in rats. *J Hepatol* 2008; 48: 289–99.
11 Hijikawa T, Kaibori M, Uchida Y *et al.* Insulin-like growth factor-I prevents liver injury through the inhibition of TNF-α and iNOS induction in d-galactosamine and lipopolysaccharide-treated rats. *Shock* 2008; 29: 740–7.
12 Ishizaki M, Kaibori M, Uchida Y *et al.* Protective effect of FR183998, a Na^+/H^+ exchanger inhibitor, and its inhibition of iNOS induction in hepatic ischemia-reperfusion injury in rats. *Shock* 2008; 30: 311–17.
13 Nakanishi H, Kaibori M, Teshima S *et al.* Pirfenidone inhibits the induction of iNOS stimulated by interleukin-1β at a step of NF-kB DNA binding in hepatocytes. *J Hepatol* 2004; 41: 730–6.
14 Yoshida H, Kwon A-H, Kaibori M *et al.* Edaravone prevents iNOS expression by inhibiting its promoter transactivation and mRNA stability in cytokine-stimulated hepatocytes. *Nitric Oxide Biol Chem* 2008; 18: 105–12.
15 Kanemaki T, Kitade H, Hiramatsu Y, Kamiyama Y, Okumura T. Stimulation of glycogen degradation by prostaglandin E2 in primary cultured rat hepatocytes. *Prostaglandins* 1993; 45: 459–74.
16 Seglen PO. Preparation of isolated rat liver cells. *Methods Cell Biol* 1976; 13: 29–83.
17 Horiuti Y, Ogishima M, Yano K, Shibuya Y. Quantification of cell nuclei isolated from hepatocytes by cell lysis with nonionic detergent in citric acid. *Cell Struct Funct* 1991; 16: 203–7.
18 Green LC, Wagner DA, Glogowski J, Skipper PL, Wishnok JS, Tannenbaum SR. Analysis of nitrate, nitrite and [15N]nitrate in biological fluids. *Anal Biochem* 1982; 126: 131–8.
19 Chomczynski P, Sacchi N. Single-step method of RNA isolation by acid guanidinium thiocyanate-phenol-chloroform extraction. *Anal Biochem* 1987; 162: 156–9.
20 Nishizawa M, Nakajima T, Yasuda K *et al.* Close kinship of human 20alpha-hydroxysteroid dehydrogenase gene with three aldo-keto reductase genes. *Genes Cells* 2000; 5: 111–25.
21 Unezaki S, Nishizawa M, Okuda-Ashitaka E *et al.* Characterization of the isoforms of MOVO zinc finger protein, a mouse homologue of *Drosophila Ovo*, as transcription factors. *Gene* 2004; 336: 47–58.
22 Schreiber E, Matthias P, Müller MM, Schaffner W. Rapid detection of octamer binding proteins with mini-extracts, prepared from a small number of cells. *Nucleic Acids Res* 1989; 17: 6419.
23 Oda M, Sakitani K, Kaibori M, Inoue T, Kamiyama Y, Okumura T. Vicinal dithiol-binding agent, phenylarsine oxide, inhibits iNOS gene expression at a step of NF-κB DNA binding in hepatocytes. *J Biol Chem* 2000; 275: 4369–73.
24 Bradford MM. A rapid and sensitive method for the quantitation of microgram quantities of protein utilizing the principle of protein-dye binding. *Anal Biochem* 1976; 72: 248–54.
25 Matsui K, Kawaguchi Y, Ozaki T *et al.* Effect of active hexose correlated compound on the production of nitric oxide in hepatocytes. *JPEN J Parenter Enteral Nutr* 2007; 31: 373–81.
26 Inoue T, Kwon A-H, Oda M *et al.* Hypoxia and heat inhibit inducible nitric oxide synthase gene expression by different mechanisms in rat hepatocytes. *Hepatology* 2000; 32: 1037–44.
27 Kitade H, Sakitani K, Inoue K *et al.* Interleukin-1β markedly stimulates nitric oxide formation in the absence of other cytokines or lipopolysaccharide in primary cultured rat hepatocytes, but not in Kupffer cells. *Hepatology* 1996; 23: 797–802.
28 Sakitani K, Nishizawa M, Inoue K, Masu Y, Okumura T, Ito S. Synergistic regulation of inducible nitric oxide synthase gene by CCAAT/enhancer-binding protein b and nuclear factor-κB in hepatocytes. *Genes Cells* 1998; 3: 321–30.

29 Yamada M, Nishizawa M, Nakatake R *et al.* Characterization of alternatively spliced isoforms of the type I interleukin-1 receptor on iNOS induction in rat hepatocytes. *Nitric Oxide Biol Chem* 2007; 17: 98–105.
30 Kleinert H, Pautz A, Linker K, Schwarz PM. Regulation of the expression of inducible nitric oxide synthase. *Eur J Pharmacol* 2004; 500: 255–66.
31 Akira S, Kishimoto T. NF-IL6 and NF-kB in cytokine gene regulation. *Adv Immunol* 1997; 65: 1–46.
32 Teshima S, Nakanishi H, Nishizawa M *et al.* Up-regulation of IL-1 receptor through PI3K/Akt is essential for the induction of iNOS gene expression in hepatocytes. *J Hepatol* 2004; 40: 616–23.
33 Pautz A, Linker K, Hubrich R, Korhonen R, Altenhofer S, Kleivert H. The polypyrimidine tract-binding protein (PTB) is involved in the post-transcriptional regulation of human inducible nitric oxide synthase expression. *J Biol Chem* 2006; 281: 32294–302.
34 Matsui K, Nishizawa M, Ozaki T *et al.* Natural antisense transcript stabilizes inducible nitric oxide synthase mRNA in rat hepatocytes. *Hepatology* 2008; 47: 686–97.
35 Araki Y, Matsumiya M, Matsuura T *et al.* Sivelestat suppresses iNOS gene expression in proinflammatory cytokine-stimulatied hepatocytes. *Dig Dis Sci* 2011; 56: 1672–81.
36 Kawai K, Yokoyama Y, Kokuryo T, Watanabe K, Kitagawa T, Nagino M. Inchinkoto, an herbal medicine, exerts beneficial effects in the rat liver under stress with hepatic ischemia-reperfusion and subsequent hepatectomy. *Ann Surg* 2010; 251: 692–700.
37 Akao T, Kobayashi K, Aburada M. Enzymic studies on the animal and intestinal bacterial metabolism of geniposide. *Biol Pharm Bull* 1994; 17: 1573–6.

原発巣のmRNA発現からみた切除不能大腸癌肝転移に対するmFOLFOX6療法の効果予測

石橋敬一郎[*1] 岡田 典倫[*1] 田島 雄介[*1] 石 畝 亨[*1] 桑原 公亀[*1]
大澤 智徳[*1] 隈元 謙介[*1] 辻 美 隆[*1] 芳賀 紀裕[*1] 岩間 毅夫[*1]
石田 秀行[*1] 小野内常子[*2] 屋嘉比康治[*3]

〔*Jpn J Cancer Chemother* 38(12): 2220-2223, *November*, 2011〕

Prediction of the Efficacy of Modified FOLFOX6 Therapy According to the mRNA Levels of Thymidylate Synthase (TS), Excision Repair Cross-Complementing-1 and -2 (ERCC-1 and ERCC-2) and Methylenetetrahydrofolate Dehydrogenase (MTHFD) in the Primary Lesion of Colorectal Cancer: Keiichiro Ishibashi[*1], Norimichi Okada[*1], Yusuke Tajima[*1], Toru Ishiguro[*1], Kouki Kuwabara[*1], Tomonori Ohsawa[*1], Kensuke Kumamoto[*1], Yoshitaka Tsuji[*1], Norihiro Haga[*1], Takeo Iwama[*1], Hideyuki Ishida[*1], Tsuneko Onouchi[*2] and Koji Yakabi[*3] ([*1]*Dept. of Digestive Tract and General Surgery, Saitama Medical Center, Saitama Medical University*, [*2]*Teikyo University Chiba Medical Center*, [*3]*Dept. of Gastroenterology and Hepatology, Saitama Medical Center, Saitama Medical University*)

Summary

The aim of this study was to determine whether mRNA levels of thymidylate synthase (TS), excision repair cross-complementing-1 (ERCC-1), excision repair cross-complementing-2 (ERCC-2) and methylenetetrahydrofolate dehydrogenase (MTHFD) mRNA in the primary tumor could predict a tumor response in patients with unresectable liver metastasis from colorectal cancer treated with mFOLFOX6 therapy as a first-line treatment. Eighteen patients with unresectable liver metastasis from colorectal cancer treated with mFOLFOX6 therapy as a first-line treatment were enrolled in this study. There were no significant differences between the response rate and these enzymes mRNA levels. In ERCC-1 and MTHFD mRNA expression, the progression-free survival time tended to be longer in patients with low levels than in patients with high levels (ERCC-1: $p=0.08$, MTHFD: $p=0.07$). The progression-free survival time was significantly longer in patients with both ERCC-1 and MTHFD mRNA were low levels than in patients with other ($p=0.03$). The levels of ERCC-1 and MTHFD were low in patients who could perform a conversion therapy. There were no significant differences between an overall survival time and these enzymes mRNA levels. In this study, the ERCC-1 and MTHFD mRNA expression may be useful for the prediction of progression-free survival time in patients with unresectable liver metastasis from colorectal cancer treated with mFOLFOX6 therapy. Key words: Colorectal cancer, Thymidylate synthase (TS), Excision repair cross-complementing-1 (ERCC-1), Excision repair cross-complementing-2 (ERCC-2), Methylenetetrahydrofolate dehydrogenase (MTHFD)

要旨 大腸癌切除不能肝転移に対し，一次治療としてmFOLFOX6療法を施行した18例を対象に，原発巣のthymidylate synthase (TS)，excision repair cross-complementing-1 (ERCC-1)，ERCC-2，methylenetetrahydrofolate dehydrogenase (MTHFD) の各酵素のmRNA発現から，mFOLFOX6療法の効果が予測可能か検討した。奏効率と各酵素のmRNA発現の多寡には関連はなかった。無増悪生存期間は，ERCC-1低発現 ($p=0.08$)，MTHFD低発現 ($p=0.07$) で延長する傾向があった。ERCC-1，MTHFD mRNAがともに低発現と，少なくとも一方が高発現を比較すると，ともに低発現のほうが無増悪生存期間が有意に延長していた ($p=0.03$)。各酵素の発現の多寡は全生存期間と関連はなかった。conversion therapyに移行できた3例では，ERCC-1，MTHFD mRNAともに低発現であった。原発巣のERCC-1およびMTHFD mRNAを検索することは，肝転移に対するmFOLFOX6療法の効果予測に有用であることが示唆された。

[*1] 埼玉医科大学総合医療センター・消化管・一般外科
[*2] 帝京大学ちば総合医療センター・共同研究室
[*3] 埼玉医科大学総合医療センター・消化器・肝臓内科

連絡先: 〒350-8550 川越市鴨田1981 埼玉医科大学総合医療センター・消化管・一般外科
石橋敬一郎

はじめに

分子標的薬を含めた新規抗癌剤の導入が切除不能肝転移の切除率を向上させるようになってきている(conversion therapy)[1,2]。原発巣から基軸レジメンの治療効果関連因子を解析し，肝転移の治療効果を予測することが可能であれば，臨床的な意義は大きい。今回，肝転移以外に転移を認めないStage IV・再発大腸癌肝転移に対し，一次治療としてmFOLFOX6療法を施行した症例を対象に，原発巣のthymidylate synthase（TS），excision repair cross-complementing-1（ERCC-1），ERCC-2，methylenetetrahydrofolate dehydrogenase（MTHFD）の各酵素のmRNA発現から，mFOLFOX6療法の効果が予測可能か検討したので報告する。

I. 対象・方法

対象: 当科で2005年12月～2007年12月の間に，肝転移巣のみが切除不能因子であるStage IV・再発大腸癌に対し，一次治療としてmFOLFOX6療法を施行した症例のうち，原発巣のTS，ERCC-1，ERCC-2，MTHFD mRNA発現を検討し得た18例を対象とした。

患者背景: 年齢は67（33～84）歳，男性13例，女性5例。mFOLFOX6療法の投与回数は9.5（4～24）回，oxaliplatinのrelative dose intensityは81.4（64.2～100）%，腫瘍縮小効果はCR 1例，PR 5例，SD 6例，PD 6例であった（奏効率33%）。mFOLFOX6施行後，肝転移に対しR0切除が施行し得たのは3例（17%）であった。二次治療は11例（61%）に施行され，内訳はFOLFIRI 9例，FOLFIRI＋bevacizumab 2例であった（表1）。

mRNA発現: 手術時に採取した大腸癌組織からtotal RNAを抽出し，4 μgからcDNAを合成した。TS，ERCC-1，ERCC-2，MTHFD mRNA発現をreal time PCR法で定量した。内部標準として，18srRNAを用いた。各因子について中央値をcutoffとして，高発現群，低発現群の2群に分け，奏効率，無増悪生存期間，全生存期間について比較検討した。

材料の保管・利用に関し，患者自身から文書による同意を得た。本研究は埼玉医科大学および埼玉医科大学総合医療センター倫理委員会の承認の下に行われた。

統計: 連側変数は中央値（範囲）で記載した。2群間の比較にはχ^2検定またはFischerの直接確率法を用いた。生存率はKaplan-Meier法に従って算出し，生存期間の比較にはlogrank testを用いた。$p<0.05$を有意差ありとした。

II. 結　果

mRNA発現: 各因子のmRNA発現は，TS: 4.5×10^{-3}（1.1×10^{-4}～7.9×10^{-2}），ERCC-1: 1.0×10^{-2}（1.0×10^{-5}～8.4×10^{-2}），ERCC-2: 1.1×10^{-2}（4.0×10^{-4}～1.3×10^{-1}），MTHFD: 1.4×10^{-3}（1.0×10^{-5}～1.7×10^{-2}）であった。

奏効率: 各酵素mRNA発現の多寡と奏効率に関連は認めなかった（TS: $p=0.62$，ERCC-1: $p>0.99$，ERCC-2: $p=0.62$，MTHFD: $p=0.62$），（表2）。

無増悪生存期間: TS，ERCC-2 mRNA発現の多寡と無増悪生存期間に関連は認めなかった（TS: $p=0.48$，ERCC-2: $p=0.55$）。ERCC-1 mRNA発現では，中央値が高発現群で4.8か月，低発現群で9.9か月であり，低発現群のほうが良好な傾向であった($p=0.08$)。MTHFD mRNA発現では中央値が高発現群で5.3か月，低発現群が10.7か月であり，低発現群のほうが良好な傾向であった（$p=0.07$），（図1）。また，ERCC-1，MTHFDともに低発現（n=7）の中央値は13.5か月，ERCC-1，MTHFDの少なくとも一方が高発現（n=11）の中央値

表1 患者背景

性別	男性	13
	女性	5
年齢（歳）*		67（33～84）
mFOLFOX6投与回数*		9.5（4～24）
Relative dose intensity（%）*		81.4（64.2～100）
腫瘍縮小効果	CR	1 } 6（33.3%）
	PR	5
	SD	6
	PD	6
化学療法後手術		3
二次治療	FOLFIRI	9
	FOLFIRI＋bevacizumab	2

*: median（range）

表2 奏効率と各因子の発現との関係

	TS			ERCC-1	
	低値群	高値群		低値群	高値群
CR/PR	4	2	CR/PR	3	3
SD/PD	5	7	SD/PD	6	6
	$p=0.62$			$p>0.99$	

	ERCC-2			MTHFD	
	低値群	高値群		低値群	高値群
CR/PR	4	2	CR/PR	4	2
SD/PD	5	7	SD/PD	5	7
	$p=0.62$			$p=0.62$	

は5.3か月で，ERCC-1，MTHFDともに低発現のほうが有意に良好であった（p=0.03），（図2a）。

全生存期間: 各mRNA発現の多寡と，全生存期間には関連を認めなかった（TS: p=0.75，ERCC-1: p=0.47，ERCC-2: p=0.90，MTHFD: p=0.75），（図3）。また，ERCC-1，MTHFDともに低発現（n=7）の全生存期間中央値は44.5か月，ERCC-1，MTHFDの少なくとも一方が高発現（n=11）の中央値は14.4か月であり（p=0.11），ともに低発現のほうが良好な傾向であった（図2b）。

肝転移切除移行例: 肝転移巣に対し，R0切除が行われた3症例の各酵素のmRNA発現を表3に示す。いずれもERCC-1，MTHFDともに低発現であった。

Ⅲ．考　察

われわれは，2005年12月より切除不能・再発大腸癌に対して，一次治療としてmFOLFOX6療法を施行してきた[3]。これらのベースとなる5-FUの代謝経路に関連する酵素群の一つであるTS，葉酸代謝に関係するMTHFD，さらにoxaliplatinの効果に関連するDNA除去修復酵素であるERCC-1，ERCC-2について，原発巣におけるmRNA発現から肝転移巣の治療効果が予測可能か検討したところ，TSとMTHFDのmRNAが低発現であると，無増悪生存期間が延長することが判明した。

Shirotaら[4]は二次治療として，5-FU/oxaliplatinを含むレジメンを施行したStage Ⅳ・大腸癌を対象として，治療効果と原発巣の癌細胞のTS，ERCC-1 mRNA発現について検討したところ，TS mRNA発現，ERCC-1 mRNA発現ともに低発現であるほうが，いずれかが高発現と比較して生存期間の延長が認められたと報告している。また，Uchidaら[5]は大腸癌肝転移巣のTS，ERCC-1 mRNA発現と一次治療としてのXELOX療法の効果について検討し，TS mRNA低発現のほうが高発現より肝転移に対する奏効率が有意に高く，ERCC-1 mRNA低発現のほうが高発現より治療成功期間の延長が得られたと報告している。

今回の検討では，TS mRNA発現とmFOLFOX6の効果との関係は認められなかったが，ERCC-1 mRNA発現に関しては，過去の報告と矛盾しない結果であった。ERCC-1は，cisplatinやoxaliplatinなどの白金系抗癌剤で引き起こされるDNA障害に関与し，それらの薬剤感受性を低下させることが知られている[6]。理論的にはERCC-1が高発現の場合，oxaliplatinの効果は期待し難く，今回の結果は妥当な結果であったと考えられる。

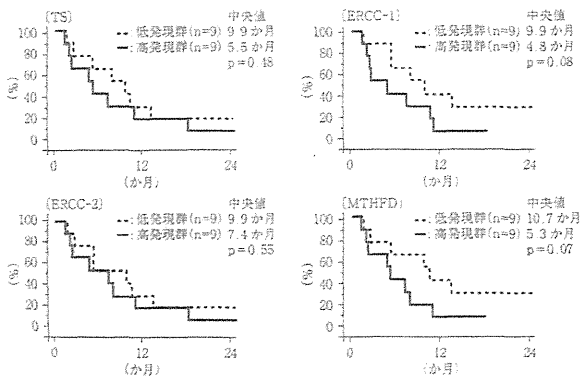

図1　無増悪生存期間

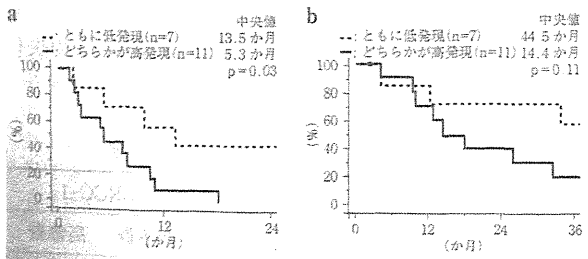

図2　ERCC-1，MTHFD mRNA発現と生存期間
a: 無増悪生存期間。b: 全生存期間。

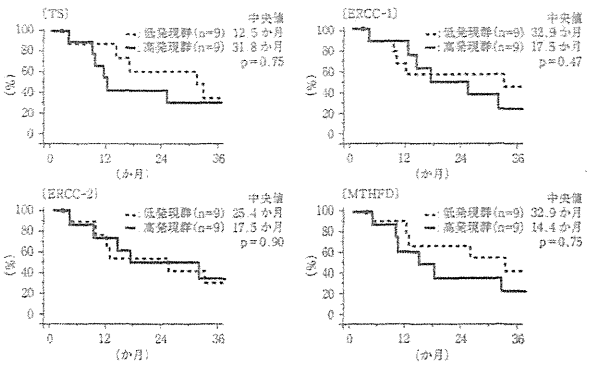

図3　全生存期間

表3　手術移行症例

症例	性別	年齢	同時性/異時性	TS	ERCC-1	ERCC-2	MTHFD
1	男性	73	異時性	低値	低値	低値	低値
2	男性	67	同時性	低値	低値	低値	低値
3	男性	67	同時性	高値	低値	高値	低値

ERCC-2もERCC-1同様に，cisplatinやoxaliplatinなどの白金系抗癌剤で引き起こされるDNA障害に関与し，それらの薬剤感受性を低下させることが知られている[6]。ERCC-1同様に，ERCC-2低発現であると，良好な治療効果が期待されるが，今回の検討ではERCC-2 mRNA発現との関連は認められなかった。MTHFD mRNA発現とmFOLFOX6の効果に関する報告は見当たらないが，MTHFDは葉酸代謝に関与するため，高発現であると5-FU/Leucovorinの効果が期待できないことが予測される[7]。今回の結果は，MTHFDの作用機序から考えると妥当な結果が得られた。いずれにしても今回の検討では症例数が少ないため，今後さらに症例を集積することと，原発巣と肝転移巣の各酵素のmRNA発現の関係についても詳しく検討する必要があると考えている。

文　献

1) Adam R, Wicherts DA, de Haas RJ, *et al*: Complete pathologic response after preoperative chemotherapy for colorectal liver metastases: myth or reality? *J Clin Oncol* **26**(10): 1635-1641, 2008.
2) Auer RC, White RR, Kemeny NE, *et al*: Predictors of a true complete response among disappearing liver metastases from colorectal cancer after chemotherapy. *Cancer* **116**(6): 1502-1509, 2010.
3) 石橋敦一郎，傍島　潤，横山　勝・他：切除不能・再発大腸癌に対するmFOLFOX6療法の使用経験．癌の臨 **53**(1): 57-63, 2007.
4) Shirota Y, Stoehlmacher J, Brabender J, *et al*: *ERCC1* and thymidylate synthase mRNA levels predict survival for colorectal cancer patients receiving combination oxaliplatin and fluorouracil chemotherapy. *J Clin Oncol* **19**(23): 4298-4304, 2001.
5) Uchida K, Danenberg PV, Danenberg KD, *et al*: Thymidylate synthase, dihydropyrimidine dehydrogenase, ERCC1, and thymidine phosphorylase gene expression in primary and metastatic gastrointestinal adenocarcinoma tissue in patients treated on a phase I trial of oxaliplatin and capecitabine. *BMC Cancer* **8**: 386, 2008.
6) Altaha R, Liang X, Yu JJ, *et al*: Excision repair cross complementing-group 1: Gene expression and platinum resistance. *Int J Mol Med* **14**(6): 959-970, 2004.
7) Kawakami K, Ruszkiewicz A, Bennett G, *et al*: DNA hypermethylation in the normal colonic mucosa of patients with colorectal cancer. *Br J Cancer* **94**(4): 593-598, 2006.

本論文の要旨は第33回日本癌局所療法研究会において発表した。

4. 大腸癌における分子標的治療
a) 切除不能大腸癌における分子標的治療*

隈元謙介　石橋敬一郎　石田秀行**

〔要旨〕近年の分子標的治療薬の開発はめざましく，切除不能大腸癌の化学療法においても抗vascular endothelial growth factor(VEGF)抗体のbevacizumabと抗epidermal growth factor receptor(EGFR)抗体のcetuximab，panitumumabの3剤がすでに治療に使われている．個々の症例において，これら分子標的治療薬をどのタイミングでどの抗癌薬と併用すれば治療効果を最大限引き出されるかは，数々の臨床試験の結果により徐々に明らかとなってきており，その結果は治療ガイドラインに反映されている．本稿では，それらエビデンスをもとに切除不能大腸癌の化学療法における各分子標的治療薬の位置づけとその治療の意義について解説する．

はじめに

近年の切除不能大腸癌に対する化学療法の変遷にはめざましい進歩があり，fluorouracil(5-FU)/leucovorin(LV)にoxaliplatinを併用したFOLFOX療法や，capecitabineにoxaliplatinを併用したCapeOX療法，また5-FU/LVにirinotecanを併用したFOLFIRI療法により，生存期間の中央値は約2年ほどと，従来の5-FU中心の治療をはるかに上回る生存期間の延長が得られるようになった．さらに，分子標的治療薬の開発がすすみ，大腸癌に対して有効性が証明されている治療薬として抗vascular endothelial growth factor(VEGF)抗体のbevacizumabと抗epidermal growth factor receptor(EGFR)抗体のcetuximab，panitumumabの3剤がすでに治療に使われている．

これら分子標的治療薬の登場により切除不能大腸癌に対する治療戦略は多様化し，個々の患者に適した治療を行うことでさらなる生存期間の延長が期待されている．実際にどのようにこれら分子標的治療薬を使い分けていくか，あるいはどのような順序で使うのかは，最新版の海外のNational Comprehensive Cancer Network(NCCN)ガイドライン[1]や，わが国の大腸癌治療ガイドライン[2]に記載されている治療アルゴリズムを参考に判断することが推奨される．

本稿では，NCCNガイドライン(図1)に記載されている切除不能大腸癌に対する一次，二次，三次治療の分子標的治療薬の治療アルゴリズムについて，これまでの第Ⅲ相臨床試験(表1)の結果をふまえて，分子標的治療薬の位置づけとその治療の意義について解説する．

キーワード：切除不能大腸癌，bevacizumab，cetuximab，panitumumab

* Molecular-targeted therapy for unresectable metastatic colorectal cancer

** K. Kumamoto(講師)，K. Ishibashi(講師)，H. Ishida(教授)：埼玉医科大学総合医療センター消化管・一般外科．

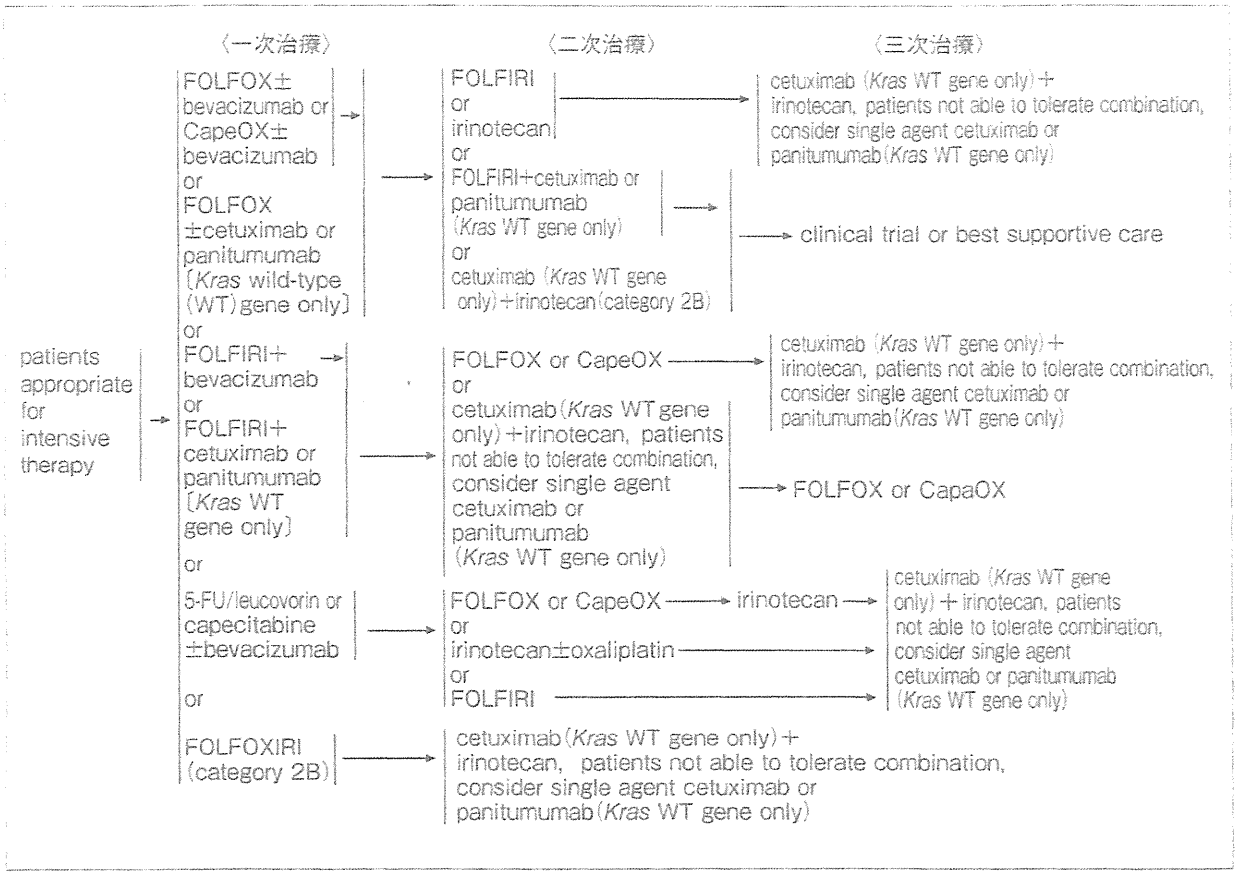

図1. NCCN治療ガイドライン(V1, 2011)切除不能大腸癌に対する化学療法(文献1より引用改変)

表1. 分子標的治療薬の有効性を示した主な第Ⅲ相臨床試験

	bevacizumab	cetuximab	panitumumab
一次治療	NO16966試験[3] (FOLFOX4/CapeOX)	OPUS試験[14] (FOLFOX4) MRC COIN試験[15] (FOLFOX/CapeOX) CRYSTAL試験[16] (FOLFIRI)	PRIME試験[17] (FOLFOX4)
二次治療	E3200試験[18] (FOLFOX4)	EPIC試験[19] (irinotecan)	20050181試験[23] (FOLFIRI)
三次治療		NCIC CTG CO.17試験[21]	20020408試験[24]

Ⅰ. 一次治療における分子標的治療薬の位置づけとその治療の意義

1. 一次治療における分子標的治療薬の現況

FOLFOX, CapeOXあるいはFOLFIRIに各分子標的治療薬を併用するレジメンが一次治療として推奨されている. Bevacizumabに関しては, その有害事象によるリスクが高いと考えられる症例以外は投与可能である. なおbevacizumabの他剤との併用について, NCCNガイドラインではFOLFOX, CapeOXとの併用は± bevacizumab, FOLFIRIでは+ bevacizumabとなっているのに対し, わが国の大腸癌治療ガイドラインではFOLFIRIとの併用でも± bevacizumabとなっている点で異なることに留意する必要がある. また, cetuximab, panitumumabは, 当初二次あるいは三次治療についてのエビデンスが主であったが, 近年一次治療としての有効性を示す報告によりその分子生物学的作用機序に基づく臨床試験の結果から, ガイドライン上*Kras*遺伝子が野生型

である症例に限定して投与が推奨されている．各々の分子標的治療薬の上乗せ効果は，これまでのさまざまなランダム化臨床試験により証明されており異論のないものである．しかしながら，FOLFOX，CapeOXあるいはFOLFIRIとbevacizumab，cetuximab，panitumumabの組み合わせにより選択肢が増え，いずれの治療薬を第一選択にすることで，奏効率や生存期間の延長において優れているかという詳細な報告はなく，実臨床でどの治療薬を選択するかは臨床医に委ねられているのが現状である．今後，各治療レジメンに対しよりよい効果を得るための適応条件が遺伝子診断などで簡便に予測できることが期待される．

2．一次治療における各分子標的治療薬の役割

a）Bevacizumab

i）FOLFOX/CapeOX ± bevacizumab

FOLFOXもしくはCapeOXにbevacizumabを加えた治療の有効性はNO16966試験[3]で明らかにされている．これは，FOLFOX4 ± bevacizumabとCapeOX ± bevacizumabの4とおりの治療デザインでFOLFOXに対するCapeOXの非劣性を検証することと，FOLFOX4もしくはCapeOXに対するbevacizumabの上乗せ効果を検証した試験である．主要評価項目である無増悪生存期間（progression-free survival：PFS）の中央値はFOLFOX/CapeOXで8.0ヵ月，bevacizumab併用群で9.4ヵ月（HR = 0.83，$p = 0.0023$）であり，bevacizumab併用により有意な延長が認められた．この1.4ヵ月のPFSの延長は，AVF2107g試験[4]〔irinotecan/5-FU/LV（IFL）vs IFL + bevacizumab〕やAVF2192g試験[5]（5-FU/LV vs 5-FU/LV + bevacizumab）のbevacizumab併用群で，PFSがそれぞれ4.4，3.7ヵ月延長した結果に比べるとやや見劣りする成績である．これはoxaliplatinによる神経毒性などにより中止となった症例が多かったことが一因である．なお，NO16966試験における全生存期間（overall survival：OS）の中央値は，FOLFOX/CapeOXで19.9ヵ月，bevacizumab併用群で21.3ヵ月（$p = 0.0769$）とbevacizumab併用により有意な延長は得られていない．これらの結果は，ガイドライン上におけるFOLFOX，CapeOXとの併用が± bevacizumabとなっている一因と思われる．

ii）FOLFIRI + bevacizumab

FOLFIRIとbevacizumabの一次治療に関して参考となるデータとしてBICC-C試験[6]があげられる．これは，未治療の切除不能大腸癌430例に対するirinotecanを軸としたFOLFIRI，IFL，CapeIRI（capecitabine + irinotecan）を比較する試験として開始されたが，前述したAVF2107g試験でIFLにbevacizumab併用の有効性が示されたことを受けて，IFL + bevacizumab（$n = 60$）とFOLFIRI + bevacizumab（$n = 57$）の比較・検討も行われた．その結果，主要評価項目であるPFSは，IFLとFOLFIRIの中央値がそれぞれ5.9ヵ月，7.6ヵ月（$p = 0.004$）とFOLFIRIが有意に優れていた．Bevacizumabを併用したIFL + bevacizumab群とFOLFIRI + bevacizumab群のPFS中央値は，それぞれ8.3ヵ月，11.2ヵ月（$p = 0.28$）で統計学的に有意差は得られなかったものの，FOLFIRI + bevacizumabのほうが良好な結果であった．さらに続報[7]により両群のOS中央値は19.2ヵ月，28.0ヵ月（$p = 0.037$）と，FOLFIRI + bevacizumab群で有意に優れた結果が得られている．

FOLFIRI + bevacizumab療法の有効性を検証した第Ⅲ相臨床試験はないが，第Ⅳ相試験としてAVIRI試験[8]やBEAT試験[9]，またBRiTE試験[10]があり，いずれもFOLFIRI + bevacizumab療法の安全性と有効性が示されている．

AVF2107g試験でIFLにbevacizumabの上乗せ効果が非常に大きかったという成績をふまえて，さらにBICC-C試験でFOLFIRI + bevacizumabのほうが優れているという結果や大規模な第Ⅳ相試験の結果から，ガイドライン上FOLFIRIには± bevacizumabではなく，+ bevacizumabと記載されていると考えられる．

iii）5-FU/LV ± bevacizumab

5-FU/LVへのbevacizumab併用による上乗せ効果は前述のAVF2192g試験[5]が根拠となる．この試験は，irinotecan不適格例〔65歳以上，performance status（PS）1もしくは2，血清アルブミン値3.5 g/dl以下，腹部骨盤への照射歴あり〕を対象に，5-FU/LV投与群と5-FU/LV + bevacizumab投与群を比較・検討した．主要評価項目であったOSの中央値は12.9ヵ月と16.6ヵ月で有意差を得られなかったが，副次評価項目である

PFS中央値は5.5ヵ月，9.2ヵ月（HR＝0.50，p＝0.0002）と5-FU/LV＋bevacizumab群で有意に優れていた．その他，同様の比較・検討をされた3試験[5,11,12]を統合し解析した結果でも，5-FU/LVにbevacizumabを加えることでPFS，OSが有意に延長されたという報告がある[13]．Oxaliplatinやirinotecanに耐えられないような症例に対して，5-FU/LV＋bevacizumabは今後も選択肢の一つとして有用なレジメンであるといえよう．

b) Cetuximab

i) FOLFOX ± cetuximab

FOLFOXにcetuximab併用の一次治療への有効性を示した報告にOPUS試験[14]がある．これは，FOLFOX4投与群とFOLFOX4＋cetuximab投与群を比較・検討したランダム化第Ⅱ相試験である．主要評価項目であるresponse rate（RR）はFOLFOX4群で36％，FOLFOX4＋cetuximab群で46％と，cetuximab併用により10％の上乗せ効果があったが，統計学的に有意差は得られなかった．*Kras*遺伝子野生型例に限定した場合のRRはFOLFOX4群で37％であったのに対し，FOLFOX4＋cetuximab群では61％と有意に高い奏効率が得られた．また，PFSも有意な延長が認められた．一方，*Kras*遺伝子変異型例ではcetuximab併用群でRR，PFSともに低下しており，cetuximab併用群ではむしろ治療効果が下がるという結果であった．このことから，ガイドラインではFOLFOX＋cetuximabの投与は*Kras*遺伝子野生型例に限定することを条件づけている．

最近，未治療の切除不能大腸癌を対象にFOLFOXとCapeOXの化学療法群，FOLFOX，CapeOXにcetuximabを併用した群に分けて，主要評価項目として*Kras*野生型患者のOSを比較・検討したMRC COIN試験[15]の結果が報告された．その結果，*Kras*野生型患者のOS中央値は化学療法群が17.9ヵ月，cetuximab併用群が17.0ヵ月であり，cetuximab併用による上乗せ効果は認められなかった．大規模試験の結果として，予想されるような*Kras*野生型患者へのcetuximabの上乗せ効果が得られなかったが，奏効率に関してcetuximab併用群で有意に高かった（p＝0.049）点はOPUS試験と同様の結果であった．サブ解析データによるとCapeOXとの併用で成績がわるかったことは，capecitabineによる消化器毒性が強くプロトコル変更が必要であったことやcetuximabとの相性がよくない可能性がある．現在のガイドラインには，FOLFOXへの併用のみでCapeOXとの併用については記載がない．

ii) FOLFIRI ± cetuximab

FOLFIRIにcetuximab併用の一次治療における有効性に関しては，CRYSTAL試験[16]の結果がガイドライン上の根拠となり重要である．EGFR陽性の切除不能大腸癌患者を対象に，FOLFIRIのみ（n＝599）とFOLFIRI＋cetuximab（n＝599）の比較・検討がなされ，主要評価項目であるPFS中央値はFOLFIRI群で8.0ヵ月，FOLFIRI＋cetuximab群で8.9ヵ月（HR＝0.85，p＝0.048）と，cetuximab併用によりわずか0.9ヵ月であるが有意に延長していた．OS中央値では，それぞれ18.6ヵ月，19.9ヵ月と差を認めなかった．RRはそれぞれ38.7％，46.9％（p＝0.004）と，cetuximab併用により高い奏効率を認めた．CRYSTAL試験で*Kras*野生型患者666例を対象に検討した結果では，PFS中央値がFOLFIRI群で8.7ヵ月，FOLFIRI＋cetuximab群で9.9ヵ月（HR＝0.68，p＝0.002），OS中央値もFOLFIRI群で20.0ヵ月，FOLFIRI＋cetuximab群で23.5ヵ月（HR＝0.796，p＝0.0094）と，cetuximab併用による有意な延長が示された．RRでもFOLFIRI群で43.2％，FOLFIRI＋cetuximab群で59.3％と，cetuximabの上乗せ効果が実証された．

c) Panitumumab —— FOLFOX ± panitumumab

Panitumumabの一次治療としての有効性を評価したPRIME試験[17]は19ヵ国133施設が参加し，未治療転移性大腸癌患者を対象にFOLFOX4投与群とFOLFOX4＋panitumumab投与群を比較した試験である．*Kras*野生型患者656例を対象に検討した結果，PFS中央値は，FOLFOX4群で8.0ヵ月，FOLFOX4＋panitumumab群で9.6ヵ月（HR＝0.80，p＝0.023）とpanitumumab併用群で有意に延長した．OS中央値はそれぞれ19.7ヵ月，23.9ヵ月（HR＝0.83，p＝0.072）であり，統計学的有意差は得られなかった．一方，*Kras*変異型患者440例を対象とした解析結果で